Spectral Characteristics and Meridional Variations of Energy Transformations during the First and Second Special Observation Periods of FGGE[1]

ERNEST C. KUNG AND HIROSHI TANAKA

Department of Atmospheric Science, University of Missouri-Columbia, Columbia, MO 65211

(Manuscript received 31 October 1983, in final form 15 March 1984)

ABSTRACT

Global features and meridional variations of spectral energy transformations are investigated for the first and second special observation periods (SOP-1 and SOP-2) of FGGE. The latitudinal distribution of the kinetic energy balance is also examined. The diagnosis presented is based on the GFDL data set.

The spectral distributions of the global transformations, $R(n)$ between the zonal mean and eddy components of the available potential energy, $M(n)$ between the zonal mean and eddy components of the kinetic energy and $C(n)$ between the available potential energy and the kinetic energy, all show specific seasonal characteristics for SOP-1 and SOP-2.

The characteristic latitudinal distributions of cell conversion $C(0)$ and eddy conversion $C(n)$ at various wavenumbers are presented with their vertical totals and latitude–height profiles. The equatorial maximum of $C(0)$ is associated with the upward motion of the Hadley cells. During SOP-1 the middle latitude maximum of eddy conversion $C(n)$ in the Northern Hemisphere is identified with the very active long waves $n = 1, 2$ and 3. During SOP-2 the pronounced $C(1)$ and $C(2)$ in the Northern Hemisphere are associated with the summer monsoon system, and the Southern Hemispheric conversion is intense in the Antarctic region at $n = 0$ and 1.

There is maximum production of the kinetic energy $-\mathbf{V}\cdot\nabla\phi$ at subtropical latitudes, with a secondary maximum at higher middle latitudes. Between these two regions of maximum production, there is a region of adiabatic destruction of kinetic energy above the lower troposphere. The convergence of the kinetic energy $-\nabla\cdot\mathbf{V}k$ is an important additional source of kinetic energy in middle latitudes. Dissipation D is at its maximum in middle latitudes. The seasonal contrast of the energy transformation is much more pronounced in the Northern Hemisphere than in the Southern Hemisphere, leading to more intense global energy processes during SOP-1 than SOP-2.

1. Introduction

One pertinent concern in studies of the energetics of the global atmospheric circulation is the variability of energy parameters in the space and time domains. The energetics approach is concerned with processes in which a portion of the atmospheric energy is utilized to maintain and regulate the global circulation and, simultaneously, to control growth and decay of synoptic systems. Thus, the knowledge of such variability is desirable when applying the energetics approach beyond what is observed with the global mean integrals.

In our preceding paper (Kung and Tanaka, 1983), a gross energy analysis was presented with Level IIIb data sets from the First GARP (Global Atmospheric Research Programme) Global Experiment (FGGE) for the first and second special observation periods (SOP-1 and SOP-2). Among the results presented, it was revealed that a notable contrast between the Northern and Southern Hemispheres exists in most spectral components of the available potential energy and the kinetic energy. Further, there is a significant seasonal difference in the energy reservoir of the Northern Hemisphere, whereas the difference is minor in the Southern Hemisphere. It also was suggested that the large discrepancy between this FGGE analysis and the previously available energetics estimates is largely attributable to the restriction of the earlier data coverage to the middle latitudes of the Northern Hemisphere. One subsequent topic of interest is an investigation of the hemispherical and seasonal variation of energy transformations in the proper context of global energetics.

The study reported in this paper is based on an analysis of the GFDL (Geophysical Fluid Dynamics Laboratory) version of the FGGE Level IIIb data set (Miyakoda *et al.*, 1982) during SOP-1 and SOP-2. The analysis covers the periods of 1 January–5 March 1979 and 30 April–7 July 1979 for SOP-1 and SOP-2, respectively. After a description of the analysis scheme, the spectral features of the global energy integrals are examined. Next, meridional variations of the kinetic energy balance and the energy source terms are presented with reference to the zonal mean field of motion.

[1] Contribution No. 9524, Missouri Agricultural Experiment Station.

Then, meridional variations of spectral conversion from available potential energy to kinetic energy are considered. An attempt is made throughout the paper to contrast the energetics features in the Northern and Southern Hemispheres and those during SOP-1 and SOP-2.

2. Energy equations and evaluation of energy variables

The analysis scheme was described in our preceding report (Kung and Tanaka, 1983), and only an abbreviated description of the energy equations and their evaluation is provided in this section. Symbols, definitions and variables used in this paper are listed in Table 1.

The equations of kinetic energy and available potential energy in the one-dimensional wavenumber domain, written after Saltzman (1957, 1970), are

$$\frac{\partial K_M}{\partial t} = \sum_{n=1}^{N} M(n) + C(P_M, K_M) - D(K_M), \quad (1)$$

$$\frac{\partial K(n)}{\partial t} = -M(n) + L(n) + C(n) - D(n) \quad (n = 1, 2, 3\cdots), \quad (2)$$

$$\frac{\partial P_M}{\partial t} = -\sum_{n=1}^{N} R(n) - C(P_M, K_M) + G(P_M), \quad (3)$$

$$\frac{\partial P(n)}{\partial t} = R(n) + S(n) - C(n) + G(n) \quad (n = 1, 2, 3\cdots). \quad (4)$$

The variables in Eqs. (1)–(4) follow the definitions of Saltzman (1970). Equations of the eddy kinetic energy and eddy available potential energy can be obtained by summing Eqs. (2) and (4) from $n = 1$ to N, giving

$$\frac{\partial K_E}{\partial t} = -M(K_E, K_M) + C(P_E, K_E) - D(K_E), \quad (5)$$

$$\frac{\partial P_E}{\partial t} = R(P_M, P_E) - C(P_E, K_E) + G(P_E). \quad (6)$$

Equations (1)–(6) state the balance requirement over the total mass of the atmosphere.

If the kinetic energy equation is averaged zonally with respect to longitude, it may be written as

$$\frac{\partial \bar{k}}{\partial t} = -\nabla\cdot\overline{\mathbf{V}k} - \frac{\partial\overline{\omega k}}{\partial p} - \overline{\mathbf{V}\cdot\nabla\phi} - D, \quad (7)$$

where

$$k = \frac{1}{2}(u^2 + v^2). \quad (8)$$

The production term may be considered as a summation of three process terms,

$$-\overline{\mathbf{V}\cdot\nabla\phi} = -\overline{\nabla\cdot\mathbf{V}\phi} - \frac{\partial\overline{\omega\phi}}{\partial p} - \overline{\omega\alpha}. \quad (9)$$

TABLE 1. List of symbols, definitions and variables.

p	Pressure
t	Time
u	Eastward wind component
v	Northward wind component
$\mathbf{V}$	Horizontal wind vector
k	Kinetic energy per unit mass
m	Mass of the atmosphere
α	Specific volume
ω	Vertical p-velocity (dp/dt)
ϕ	Geopotential
∇	Horizontal del operator along an isobaric surface
$\bar{q}$	Zonal average of an arbitrary function q
q'	Departure of q from zonal average
$\bar{q}''$	Departure of $\bar{q}$ from global average
n	Zonal wavenumber
N	Maximum zonal wavenumber
K	Kinetic energy
K_M	Zonal mean kinetic energy
K_E	Zonal eddy kinetic energy
$K(n)$	K at wavenumber n
P	Available potential energy
P_M	Zonal mean available potential energy
P_E	Zonal eddy available potential energy
$P(n)$	P at wavenumber n
$M(K_E, K_M)$	Transfer from K_E to K_M
$M(n)$	Transfer of $K(n)$ to K_M
$L(n)$	Transfer of K_E from all other wavenumbers to $K(n)$
$C(P, K)$	Conversion from P to K
$C(P_M, K_M)$	Conversion from P_M to K_M
$C(P_E, K_E)$	Conversion from P_E to K_E
$C(n)$	Conversion of $P(n)$ to $K(n)$
$R(P_M, P_E)$	Transfer of P_M to P_E
$R(n)$	Transfer of P_M to $P(n)$
$S(n)$	Transfer of P_E from all other wavenumbers to $P(n)$
D	Dissipation of k
$D(K_M)$	Dissipation of K_M
$D(K_E)$	Dissipation of K_E
$D(n)$	Dissipation of $K(n)$
$G(P_M)$	Generation of P_M
$G(P_E)$	Generation of P_E
$G(n)$	Generation of $P(n)$
$\partial k/\partial t$	Local time change of kinetic energy
$-\nabla\cdot\mathbf{V}k$	Horizontal flux convergence of kinetic energy
$-\partial\omega k/\partial p$	Vertical flux convergence of kinetic energy
$-\mathbf{V}\cdot\nabla\phi$	Production of kinetic energy by cross-isobaric motion
$-\nabla\cdot\mathbf{V}\phi$	Horizontal flux convergence of potential energy
$-\partial\omega\phi/\partial p$	Vertical flux convergence of potential energy
$-\omega\alpha$	Baroclinic conversion from P to K
$-\omega'\alpha'$	Conversion by eddy convection
$-\bar{\omega}''\bar{\alpha}''$	Conversion by mean meridional circulation

The original FGGE Level IIIb GFDL data sets (for the periods 1 January–5 March 1979 and 30 April–7 July 1979) were interpolated to the 4 × 5° latitude–longitude grid from 90°S to 90°N and from 0 to 355°E by Kung and Tanaka (1983). These data constitute the basic input for the computational analysis of this study. The basic input data include twice-daily values for geopotential height, humidity, temperature, wind and vertical velocity at 1000, 850, 700, 500, 400, 300, 250, 200, 150, 100 and 50 mb at 0000 and 1200 GMT. A program package from the NASA/Goddard Labo-

ratory for Atmospheric Sciences (see Baker *et al.*, 1977) was modified for computation in this diagnostic study. The eddy variables in Eqs. (5) and (6) are obtained as spectral sums over wave-number n = 1–30. For computation of the variables involved in Eqs. (7) and (9), input data at the grid points are directly used to obtain grid-point values of the energy variables. In evaluating Eqs. (1)–(7), dissipation terms of the kinetic energy and generation terms of the available potential energy are obtained as residual terms to balance the respective equations.

The energy variables are presented for the mass of the atmosphere between the pressure levels. The limits of integration for the vertical totals are from the surface to 50 mb. Computation is done for each observation time. Averages of the computed variables during the first data period are taken as SOP-1 means, and those during the second data period as SOP-2 means.

3. Global energy transformation

The transfer of the zonal mean available potential energy to eddy available potential energy $R(n)$, the transfer of the eddy kinetic energy to zonal mean kinetic energy $M(n)$, and the conversion of the available potential energy to kinetic energy $C(n)$, as computed on a global basis, are shown in Fig. 1 as functions of

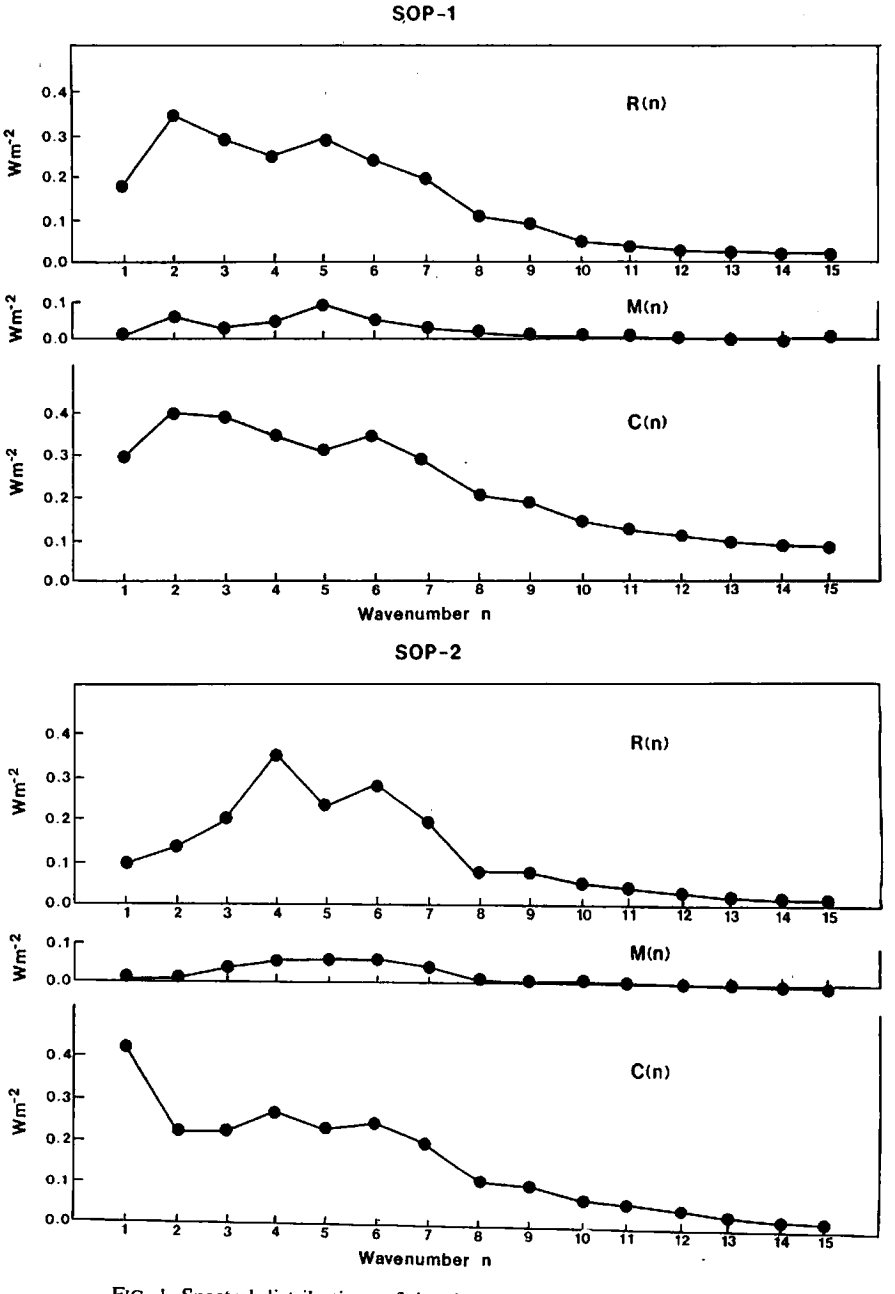

FIG. 1. Spectral distributions of the globally integrated transformations $R(n)$, $M(n)$ and $C(n)$ during SOP-1 and SOP-2.

wavenumber from $n = 1$ to 15 for SOP-1 and SOP-2. Our preceding study (Kung and Tanaka, 1983) confirms the general direction of the energy transfer in the basic energy cycle (see Lorenz, 1955), as established by earlier studies (e.g., Oort, 1964; Oort and Peixoto, 1974; Newell *et al.*, 1970; Saltzman, 1970; Wiin-Nielsen, 1968). The largest portion of the energy transformation is identified in the steps from P_M via P_E to K_E. Some K_E is further transformed to K_M as the dissipation of the kinetic energy takes place in both K_E and K_M. The spectral energy variables $R(n)$, $C(n)$ and $M(n)$ describe contributions of various sizes of zonal eddies in these steps of the energy cycle.

During SOP-1 (Fig. 1), as shown by the spectral distributions of $R(n)$ and $C(n)$, the wavenumber $n = 2$ is the most active in transferring P_M to P_E and converting P_E to K_E. The transfer of P_M to $P_E[R(n)]$ has a second peak at $n = 5$ and gradually decreases to low values at $n = 10$ and shorter. For baroclinic conversion $C(n)$, there is also a second peak at $n = 6$ which gradually decreases to low values at $n = 10$ and shorter. Most of the energy transformations by the zonal eddies take place in the long-wave and cyclone-wave ranges. For $C(n)$, however, it is noted that in the short-wave range from $n = 11$ to 15, conversion is still fairly active, consistent with generally observed synoptic activity in the atmosphere. In any case, it may be stated that during SOP-1 the long to large cyclone waves from $n = 2$ to 7 are the most active in transferring P_M to P_E and converting P_E to K_E. For the transfer from K_E to K_M, the major contribution of $M(n)$ is at $n = 4$–7. Its magnitude is far smaller than that of $R(n)$ and $C(n)$ in all spectral ranges.

In Fig. 1 a significant seasonal contrast of the spectral energy variables is apparent between SOP-1 and SOP-2. During SOP-2 the maximum of $R(n)$ is at $n = 4$–6, with a rather sharp decline at both lower and higher wavenumbers. This is apparently different from SOP-1 when a broader waverange, particularly at the longer end, is active in the transfer of P_M to P_E. The spectral distribution of baroclinic conversion during SOP-2 has a significant peak conversion at $n = 1$. From $n = 2$ to the higher wavenumbers, $C(n)$ is somewhat weaker during SOP-2 than during SOP-1; however, the eddy conversion is again not negligible even at the short end of the spectrum. During SOP-2 the spectral pattern of $M(n)$ is similar to that during SOP-1 without a noticeable deviation.

4. Meridional variations of kinetic energy balance and energy source terms

Vertical totals of the variables in the balance of the kinetic energy are listed in Table 2 for SOP-1 and SOP-2 by each latitudinal zone from 90°S to 90°N. The dissipation is obtained to balance the time change $\partial\bar{k}/\partial t$, the horizontal flux divergence $-\nabla\cdot\overline{\mathbf{V}}\overline{k}$ and the production $-\overline{\mathbf{V}}\cdot\overline{\nabla\phi}$. The vertical flux convergence

TABLE 2. Kinetic energy balance and conversion of available potential energy to kinetic energy in each 10° latitude zone during SOP-1 and SOP-2. All values are vertical totals from the surface to 50 mb. Units are W m^{-2}.

	Northern Hemisphere (°N)									Southern Hemisphere (°S)								
	90–80	80–70	70–60	60–50	50–40	40–30	30–20	20–10	10–0	0–10	10–20	20–30	30–40	40–50	50–60	60–70	70–80	80–90
SOP-1																		
$\partial\bar{k}/\partial t$	−0.1	0.0	0.1	−0.3	−0.5	0.4	−0.1	0.1	0.1	0.1	−0.1	−0.4	−0.4	−0.1	0.6	0.0	0.0	0.0
$-\overline{\mathbf{V}}\cdot\overline{\nabla\phi}$	−1.9	5.6	5.9	2.5	2.9	7.6	13.2	8.4	2.1	1.6	1.7	2.7	4.1	5.1	3.1	2.8	3.3	1.4
$-\overline{\nabla}\cdot\overline{\mathbf{V}k}$	1.9	−0.9	−0.1	2.0	2.0	3.5	−1.4	−3.3	−0.5	−0.3	−0.4	−1.3	−1.1	1.6	2.2	0.0	−0.2	−0.0
D	0.1	4.7	5.7	4.8	5.4	10.7	11.9	5.0	1.5	1.2	1.4	1.8	3.4	6.8	4.7	2.8	3.1	1.4
$-\overline{\omega''\alpha''}$	10.4	5.2	−3.4	0.5	6.8	3.2	−3.8	−3.6	9.0	14.0	9.9	0.4	−1.5	0.1	0.2	−0.4	−0.3	3.4
$-\overline{\omega}\overline{\alpha}$	−0.3	2.1	4.1	4.9	8.2	6.1	4.6	2.6	2.3	2.6	3.3	3.0	3.2	5.0	4.2	2.2	0.9	0.7
SOP-2																		
$\partial\bar{k}/\partial t$	0.0	−0.2	0.0	0.2	−0.1	−0.3	−0.4	0.0	0.1	0.1	−0.1	−0.6	0.0	0.3	0.5	0.1	−0.2	0.1
$-\overline{\mathbf{V}}\cdot\overline{\nabla\phi}$	0.8	2.5	2.0	0.6	0.8	1.5	3.9	3.0	2.1	1.9	4.0	5.2	5.1	4.5	4.0	8.3	8.9	4.4
$-\overline{\nabla}\cdot\overline{\mathbf{V}k}$	0.1	−0.7	0.6	1.3	0.8	−0.2	−0.7	−0.7	−0.2	−0.1	−1.6	−2.3	1.1	3.1	3.0	−0.9	−1.2	−0.2
D	0.9	2.0	2.6	1.7	1.7	1.6	3.6	2.3	1.8	1.7	2.5	3.5	6.2	7.3	6.5	7.3	7.9	4.1
$-\overline{\omega''\alpha''}$	1.3	2.2	−1.2	−1.0	0.5	0.4	−1.5	5.0	7.4	4.9	−1.4	−1.9	0.7	0.7	−0.4	−1.2	17.1	15.5
$-\overline{\omega}\overline{\alpha}$	0.8	1.2	1.4	1.2	2.3	4.5	3.1	2.4	1.4	1.5	0.9	1.5	3.6	3.6	3.8	3.8	6.7	3.4

$-\overline{\partial\omega k/\partial p}$ is not considered for the balance of the vertical totals.

It is shown in Table 2 that a first maximum in kinetic energy production is at subtropical to middle latitudes, with a second maximum located at higher latitudes poleward of 60° in each hemisphere. The regions of the first latitudinal maximum of $-\overline{\mathbf{V}\cdot\nabla\phi}$ in each observational period approximate the latitudes of the westerly maximum (see Figs. 2, 3 and 4). In the Southern Hemisphere during SOP-2 an extended westerly maximum region is recognized (Figs. 2 and 4), and the uniformly active $-\overline{\mathbf{V}\cdot\nabla\phi}$ is observed throughout subtropical to high latitudes. The vertical profile of the production $-\mathbf{V}\cdot\nabla\phi$ is known to have two peaks, in the lower boundary and at the jet stream level (e.g., Kung, 1967; Kung and Tanaka, 1983; Smith and Adhikary, 1974). As indicated in the latitude–height cross section of Fig. 5, the production of the kinetic energy in the lower boundary is shown to be most intense in the latitudes of the Ferrel cells, decreasing to a minimum in tropical latitudes. In the free atmosphere there are distinct regions of adiabatic destruction of kinetic energy, as shown by negative values of $-\overline{\mathbf{V}\cdot\nabla\phi}$, in the middle latitudes of both hemispheres and in the polar region of the Northern Hemisphere. Except for these negative production regions in the free atmosphere, other portions of the latitude–height cross sections are marked by positive values of $-\overline{\mathbf{V}\cdot\nabla\phi}$ with intense production in association with the westerly jets (see Fig. 2). This distribution of the production term from subtropical to high latitudes is in qualitative agreement with Kung's (1970) observation using a limited database.

The basic latitude–height patterns of $-\mathbf{V}\cdot\nabla\phi$ remain comparable through SOP-1 and SOP-2 (Fig. 5). However, the intensity of the production $-\overline{\mathbf{V}\cdot\nabla\phi}$ in the Northern Hemisphere during SOP-1 is the highest, and that of the same hemisphere during SOP-2 is the lowest. Consequently, the seasonal contrast of $-\overline{\mathbf{V}\cdot\nabla\phi}$ is significantly greater in the Northern Hemisphere than in the Southern Hemisphere, as also is observed in Table 2. This is consistent with a minor difference in the intensity of the Southern Hemisphere general circulation between the winter and summer of the International Geophysical Year, as computed by Peixoto and Corte-Real (1983), in contrast to the generally observed large seasonal difference in the Northern Hemisphere. The latter seasonal difference may

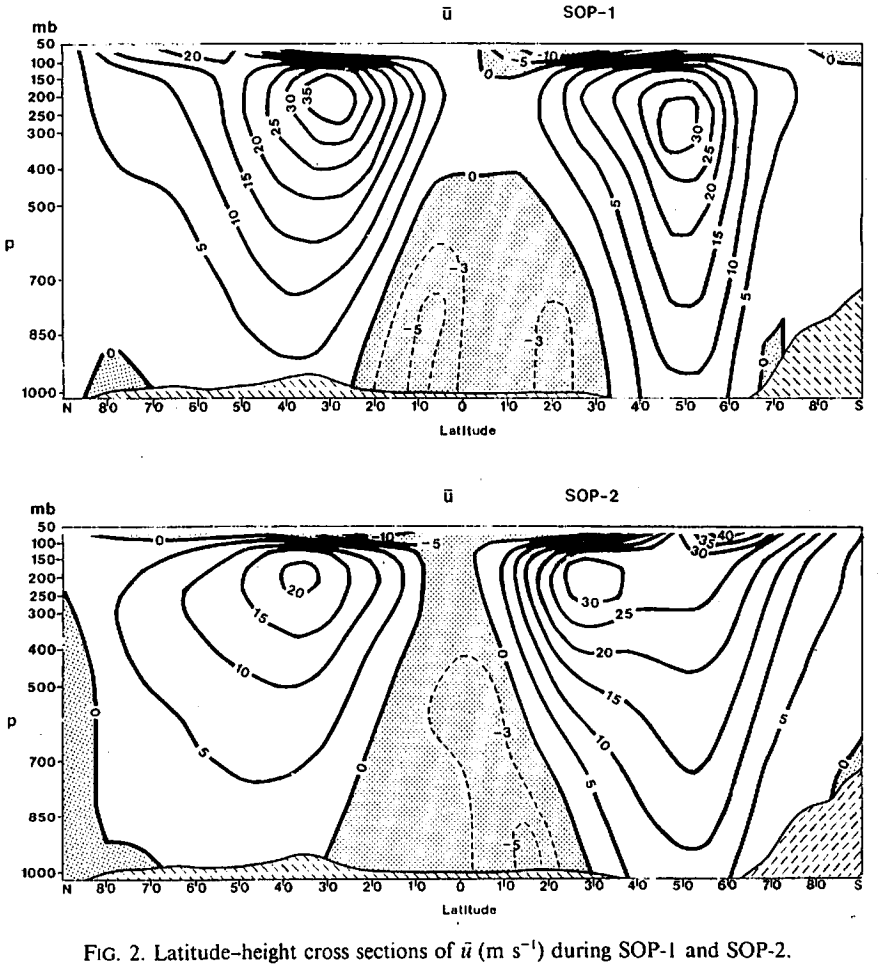

FIG. 2. Latitude–height cross sections of $\bar{u}$ (m s^{-1}) during SOP-1 and SOP-2.

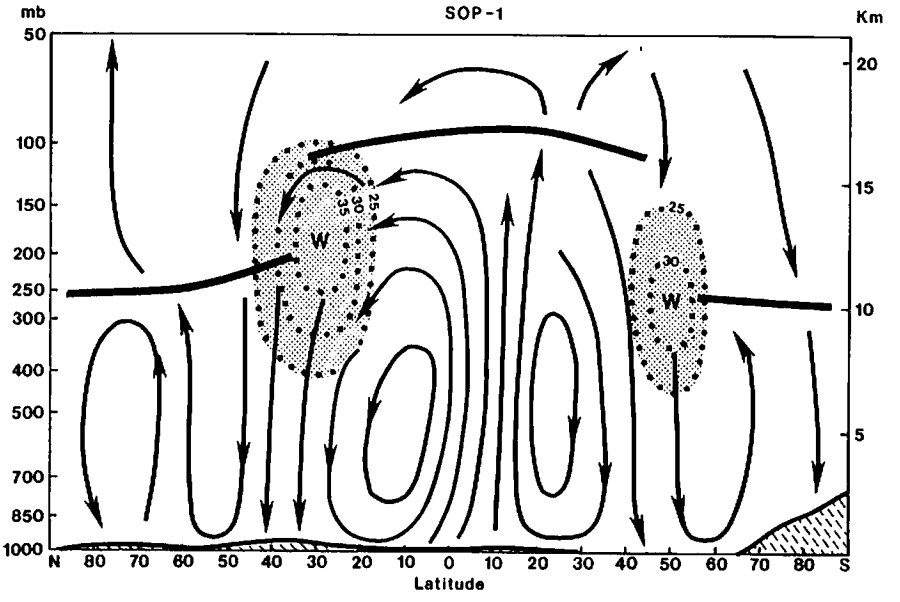

FIG. 3. Patterns of mean meridional circulation during SOP-1 constructed from $\bar{v}$ and $\bar{\omega}$. Tropopause is indicated by heavy lines. Isotachs of $\bar{u}$ in the areas of the jet stream are in units of m s^{-1}.

lead to the seasonal difference in global energetics noted by Kung and Tanaka (1983), in that both the energy level and the intensity of the general circulation are more pronounced during SOP-1 than during SOP-2.

The listing of the transport term $-\overline{\nabla \cdot \mathbf{V}k}$ in Table 2 shows that the lower latitudes of the Hadley cells export kinetic energy to middle latitudes. Convergence of kinetic energy is an important additional source of kinetic energy in middle latitudes. This is particularly true in latitudes where $-\overline{\mathbf{V} \cdot \nabla \phi}$ is small, because of adiabatic destruction of the kinetic energy in the free atmosphere. The meridional distribution of the dissipation D, like that of the production $-\overline{\mathbf{V} \cdot \nabla \phi}$, follows the position of the westerly maximum. However, the maximum of D is observed in latitudes higher than the latitudes of the subtropical maximum of $-\mathbf{V} \cdot \nabla \phi$ because of the poleward transport of kinetic energy. Dissipation in the equatorial belt is generally small. Since interhemispherical transport of kinetic energy is very limited, the above argument concerning the sea-

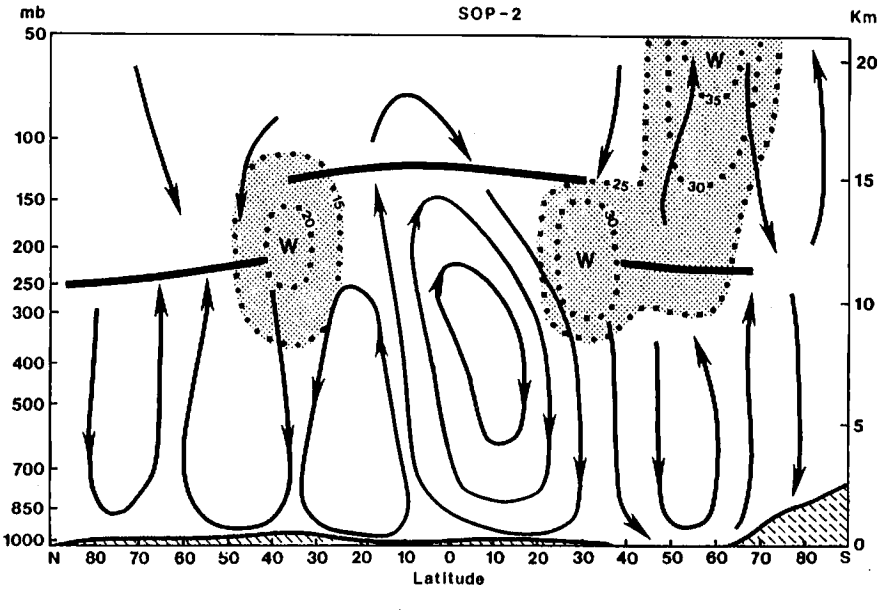

FIG. 4. As in Fig. 3, but for SOP-2.

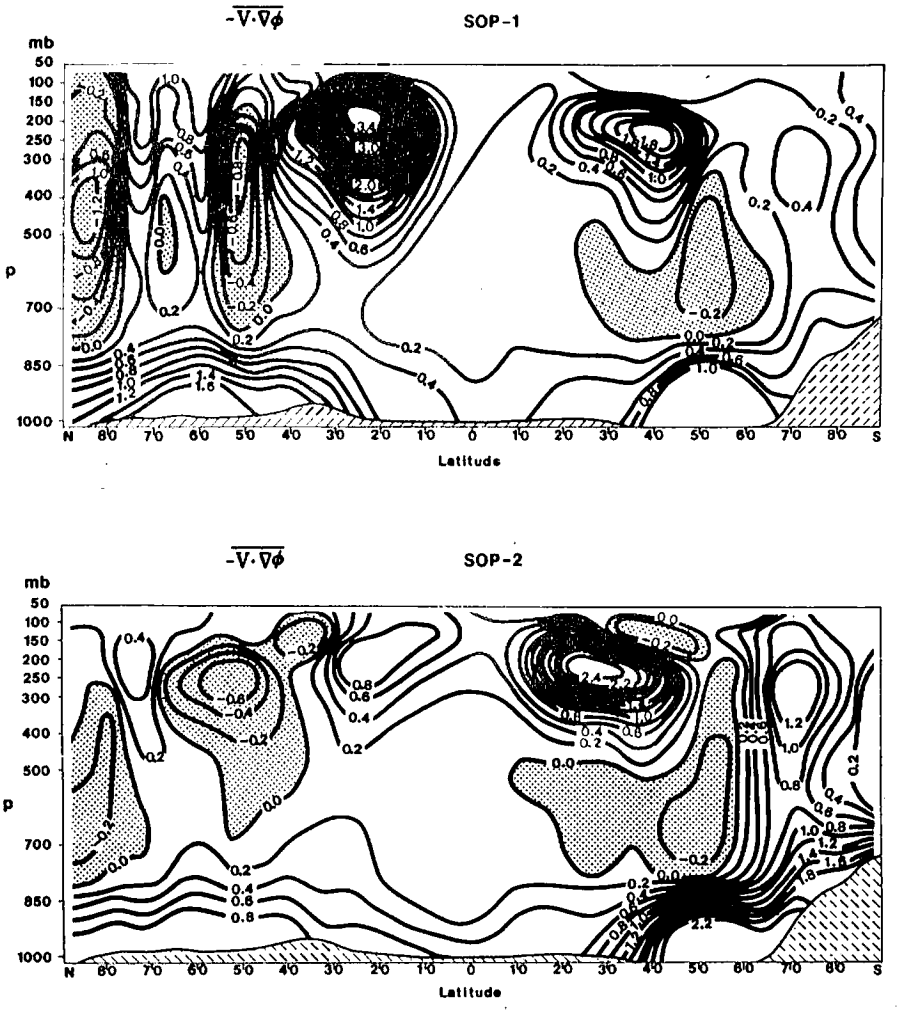

FIG. 5. Latitude-height cross sections of kinetic energy production $-\mathbf{V}\cdot\nabla\phi$ [W m^{-2} (100 mb)$^{-1}$] during SOP-1 and SOP-2.

sonal variation of production also holds for dissipation, which should approximately balance the production and transport.

If Eq. (9) for kinetic energy production is integrated over the entire mass of the atmosphere, it may be written as

$$-\int_m \overline{\mathbf{V}\cdot\nabla\phi}\,dm = -\int_m \overline{\omega\alpha}\,dm$$

$$= -\int_m \bar{\omega}''\bar{\alpha}''\,dm - \int_m \overline{\omega'\alpha'}\,dm, \quad (10)$$

where the global integrals of $-\overline{\mathbf{V}\cdot\nabla\phi}$ or $-\overline{\omega\alpha}$ measure $C(P, K)$, and those of $-\bar{\omega}''\bar{\alpha}''$ and $-\overline{\omega'\alpha'}$ measure $C(P_M, K_M)$ and $C(P_E, K_E)$, respectively. Thus, the values of $-\bar{\omega}''\bar{\alpha}''$ and $-\overline{\omega'\alpha'}$ listed in Table 2 are considered to be net contributions of the zonal mean meridional cells and eddy convections to the global baroclinic conversion in specified latitudinal zones. The values of $-\bar{\omega}''\bar{\alpha}''$ listed in Table 2 appear to be overestimated. As discussed in Kung and Tanaka (1983), the magnitude of the zonal mean field $\bar{\omega}$ in the GFDL data version appears excessive, as judged from direct computations of $-\bar{\omega}''\bar{\alpha}''$, although $\bar{\omega}$ adequately describes the position and relative strength of the mean meridional cells. Their analysis indicates that the directly computed $-\bar{\omega}''\bar{\alpha}''$ may overestimate $C(P_M, K_M)$ by a factor of 2 to 3 when the diagnosis is done with the GFDL data set. Thus, they obtained $C(P_M, K_M)$ indirectly as the difference of the global integrals of $-\overline{\mathbf{V}\cdot\nabla\phi}$ and $-\overline{\omega'\alpha'}$. Despite obvious overestimates, however, the listing of $-\bar{\omega}''\bar{\alpha}''$ in Table 2 still permits observation of the general meridional characteristics of this term. The contribution by the cell conversion $-\bar{\omega}''\bar{\alpha}''$ is at its maximum in equatorial latitudes because of the generally strong upward motion of the Hadley cells. Even considering an overestimate, the contribution of $-\bar{\omega}''\bar{\alpha}''$ is significantly larger than that of the eddy conversion $-\overline{\omega'\alpha'}$ in this belt. In the lower-latitude belt where downward motion of the Hadley cells dominates, and in the higher-latitude belt where the upward motion of the Ferrel and polar cells is recognized (see

Figs. 3 and 4), we observe negative contributions of $-\bar{\omega}''\bar{\alpha}''$; otherwise, the values of $-\bar{\omega}''\bar{\alpha}''$ are positive in all other latitudes.

It is well known that the contribution of zonal eddies in the conversion of available potential energy to kinetic energy is most intense in association with large-scale disturbances in middle latitudes (e.g., Manabe *et al.*, 1970; Newell *et al.*, 1970; Saltzman, 1970; Wiin-Nielsen, 1968). The numerical values listed in Table 2 show a meridional distribution of $-\overline{\omega'\alpha'}$ that generally confirms this understanding. The eddy conversion increases from low latitudes to a midlatitude maximum and then decreases to a high-latitude minimum. The eddy conversion in the Northern Hemisphere during SOP-1 is most intense, whereas that in the same hemisphere during SOP-1 is least intense. As in the case of $-\overline{\mathbf{V}}\cdot\overline{\nabla\phi}$, the seasonal variation of $-\overline{\omega'\alpha'}$ is much more pronounced in the Northern Hemisphere than in the Southern Hemisphere.

5. Meridional variations of spectral energy conversion

The meridional variations of the conversion of the available potential energy to kinetic energy in the wavenumber domain $C(n)$ are illustrated in Figs. 6 and 7 for SOP-1 and SOP-2 from $n = 0$ to 6. Allowing for the overestimate of $C(0)$ by a factor of 2 to 3, as previously discussed, it is still one of the most important components of the spectral conversion. The eddy conversion of the long waves $C(1)$, $C(2)$ and $C(3)$ is very active in middle latitudes of the Northern Hemisphere during SOP-1. During SOP-2 in subtropical to lower middle latitudes of the Northern Hemisphere, conversions $C(1)$ and $C(2)$ stand out. This part of the conversion is significant for the summer monsoon, considering the latitudes, scale and season. Another distinct feature of the latitudinal distribution of the conversion during SOP-2 is a large $C(0)$ and $C(1)$ in high latitudes of the Southern Hemisphere, associated with baroclinicity in the Antarctic region.

The conversion $C(n)$ at n = 3–6 during SOP-1 is apparently greater than during SOP-2 in the Northern Hemisphere. In this range, the midlatitude conversion decreases with the increase in wavenumber. In the middle latitudes of the Southern Hemisphere, however, wavenumbers 4–6 are most active, whereas 1, 2 and 3 are fairly inactive; further, they do not seem to visibly intensify during SOP-2. Indeed, the seasonal variation

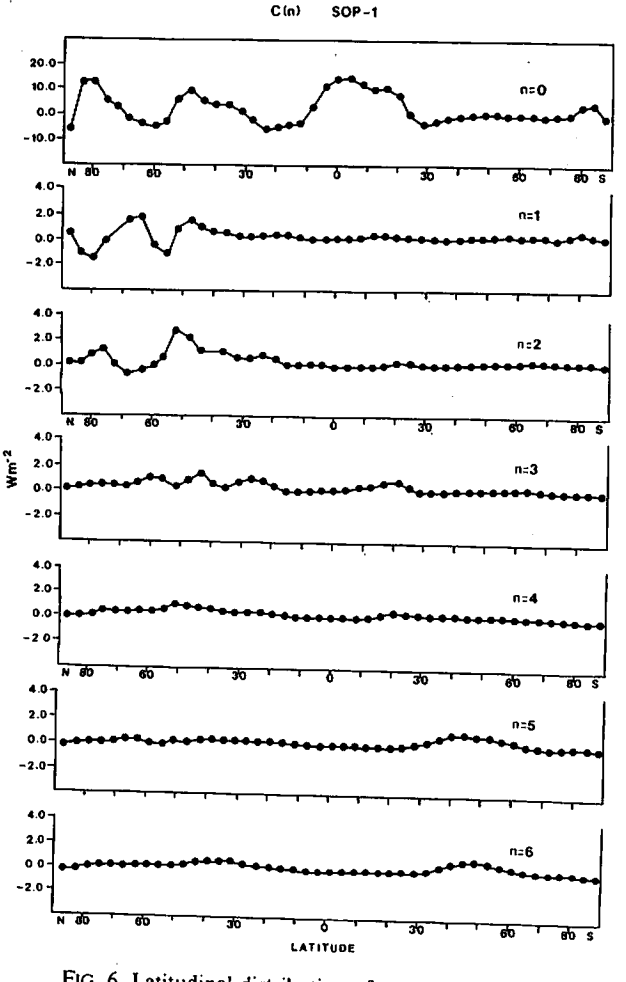

FIG. 6. Latitudinal distribution of conversion $C(n)$ from n = 0 to 6 during SOP-1.

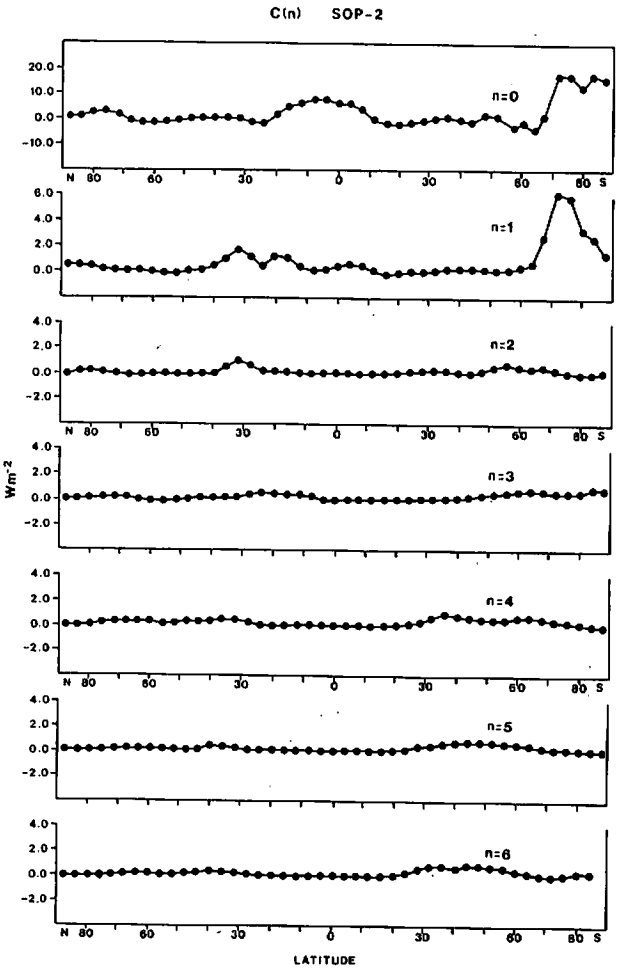

FIG. 7. As in Fig. 6, but for SOP-2.

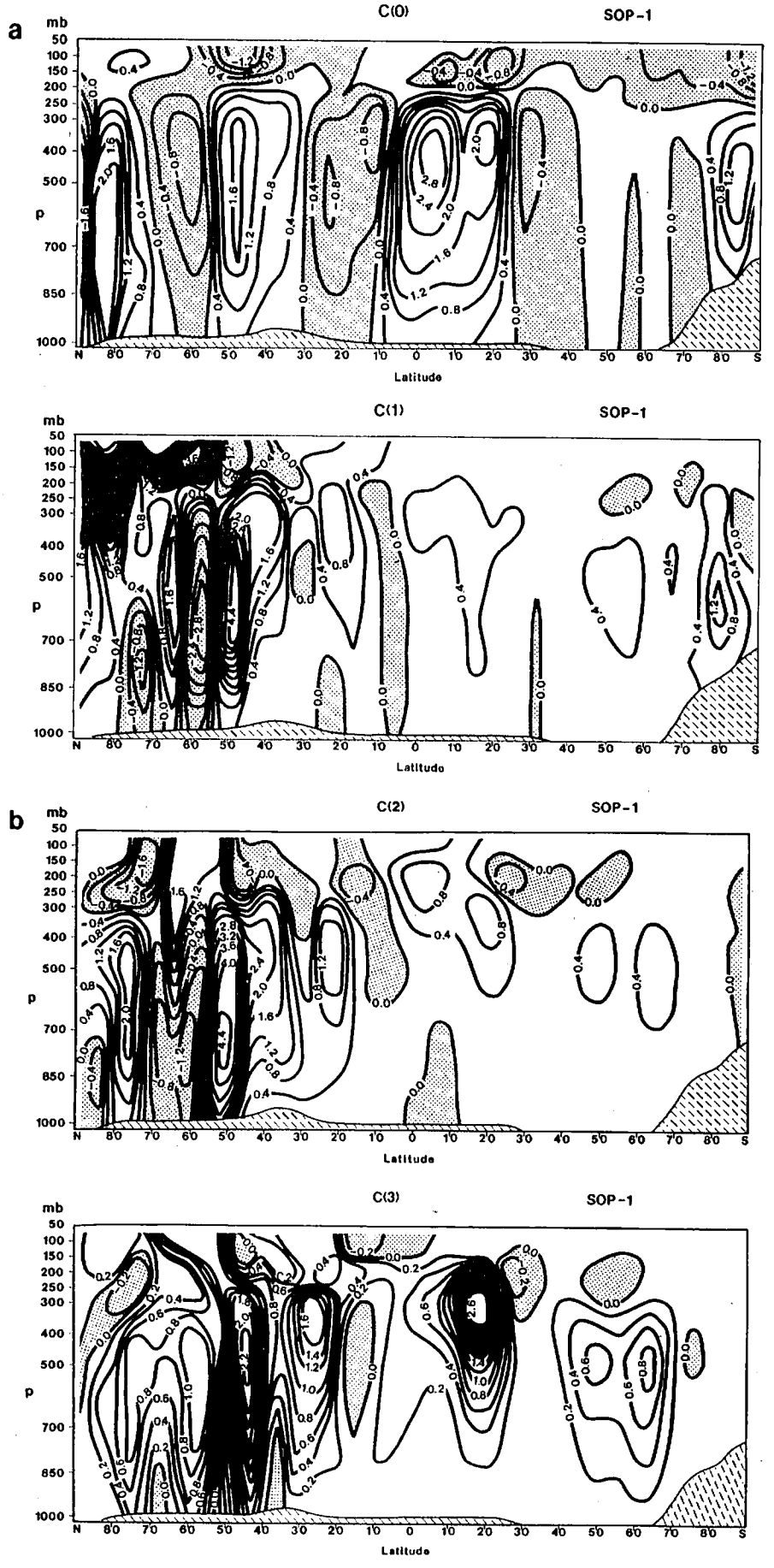

FIG. 8. Latitude–height cross sections of conversion $C(n)$ for (a) $n = 0$, (b) $n = 3$ and (c) $n = 5$ during SOP-1. $C(0)$ is in units of W m^{-2} (100 mb)$^{-1}$ and values are 10^{-1} W m^{-2} (100 mb)$^{-1}$.

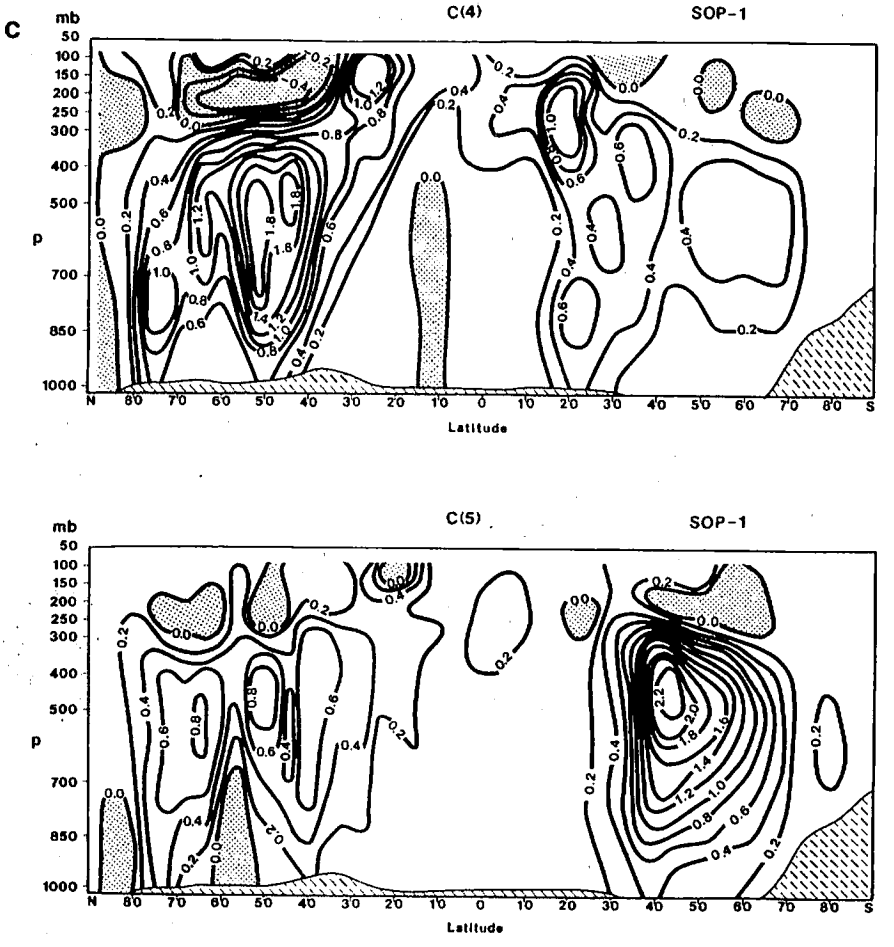

FIG. 8. (*Continued*)

of the energy conversion $C(P, K)$ in the Southern Hemisphere is mostly the contribution of the cell conversion $C(0)$, except for very long waves at Antarctic latitudes.

The latitude–height profiles of the conversion $C(n)$ at n = 0–5 during SOP-1 and SOP-2 are shown in Figs. 8 and 9. The positive and negative contributions of $C(0)$ at the different latitudes are to be decided by the departures of $\bar{\omega}$ and $\bar{\alpha}$ from their global means. Thus, in the belt of ascending motion in the Hadley cells, $C(0)$ shows a distinct positive contribution in tropical latitudes, whereas the belts of descending motion in the Hadley cells yield a negative contribution in subtropical and lower middle latitudes. The contribution of the Ferrel cells is very much dependent on the cell location (see Figs. 3 and 4) and the mean temperature of the latitude. The polar regions of both hemispheres have a significantly positive $C(0)$. Comparing $C(0)$ during SOP-1 and SOP-2, the latitudinal location of the tropical positive conversion conforms with the seasonal position of the equatorial convergence zone (Figs. 3 and 4). This positive conversion in the Hadley cells and the positive Northern Hemisphere conversion in the Ferrel and polar cells are all distinctly enhanced during SOP-1. During SOP-2 the cell conversion is much weaker at all latitudes except for the Antarctic region. There we see a heavy concentration of baroclinic conversion in $C(0)$, $C(1)$ and $C(3)$ which also appears prominent in reference to other latitudes.

In the latitude–height cross-sections of SOP-1, the eddy conversions $C(n)$ of n = 1–5 all form dominant patterns in middle latitudes of the Northern Hemisphere. The patterns are especially intense for n = 1, 2 and 3. The conversions of these very long waves are very weak in middle latitudes of the Southern Hemisphere, but increase from n = 3 to 4 and 5. At n = 5 the Southern Hemisphere has a stronger midlatitude conversion than the Northern Hemisphere. During SOP-2 in the Northern Hemisphere the intense midlatitude eddy conversions by very long waves are considerably weakened; yet, they never develop noticeably in the Southern Hemisphere. A specific feature of the Northern Hemisphere winter is the very intense eddy conversion by very long waves in middle latitudes, which are likely associated with the significant land–sea thermal contrast. The midlatitude eddy conversions in the Southern Hemisphere during SOP-2 are pronounced at n = 4 and 5. The latitude–height cross sections of $C(n)$ beyond n = 6 are not illustrated. They are, however, clearly identifiable up to n = 11 for

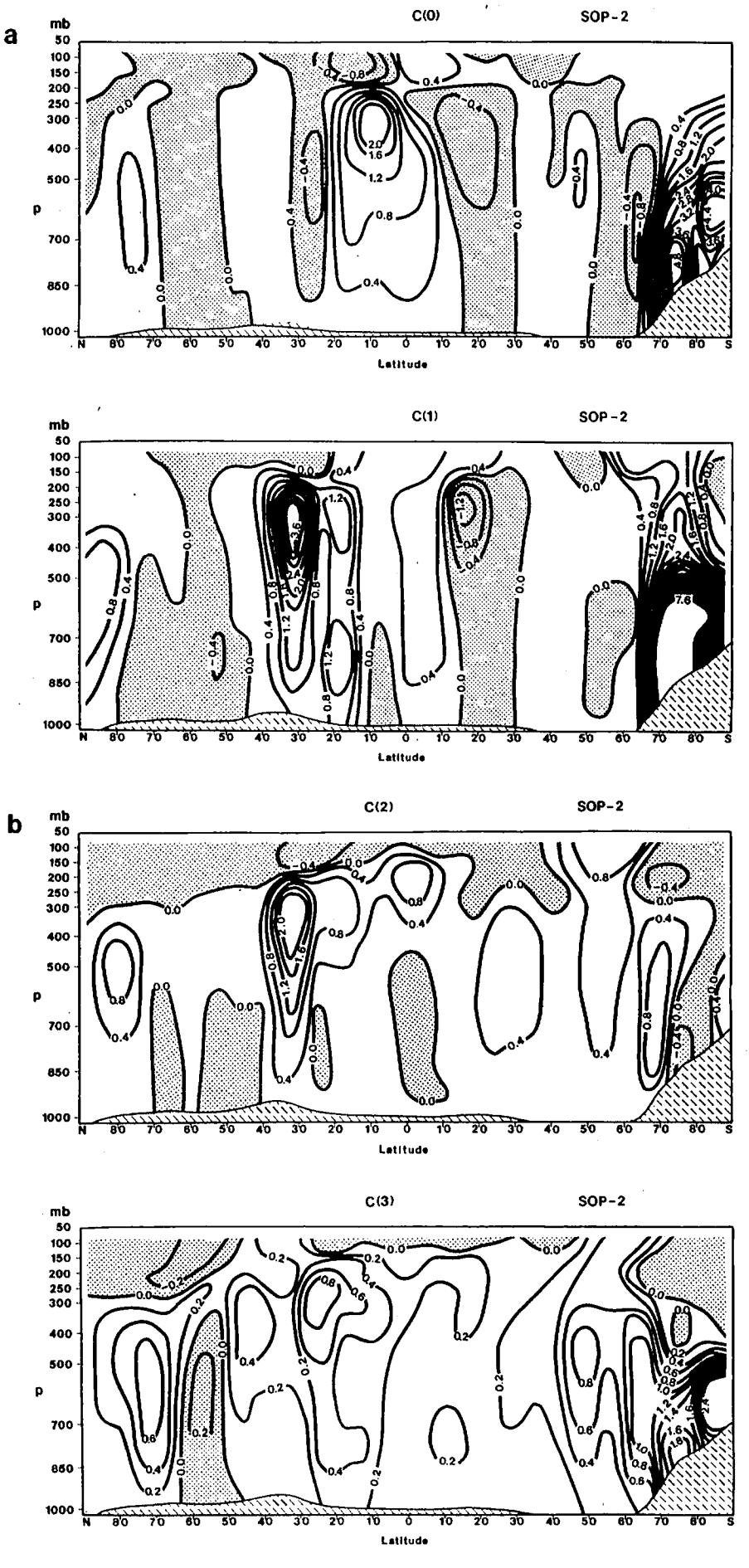

FIG. 9. As in Fig. 8, but for SOP-2.

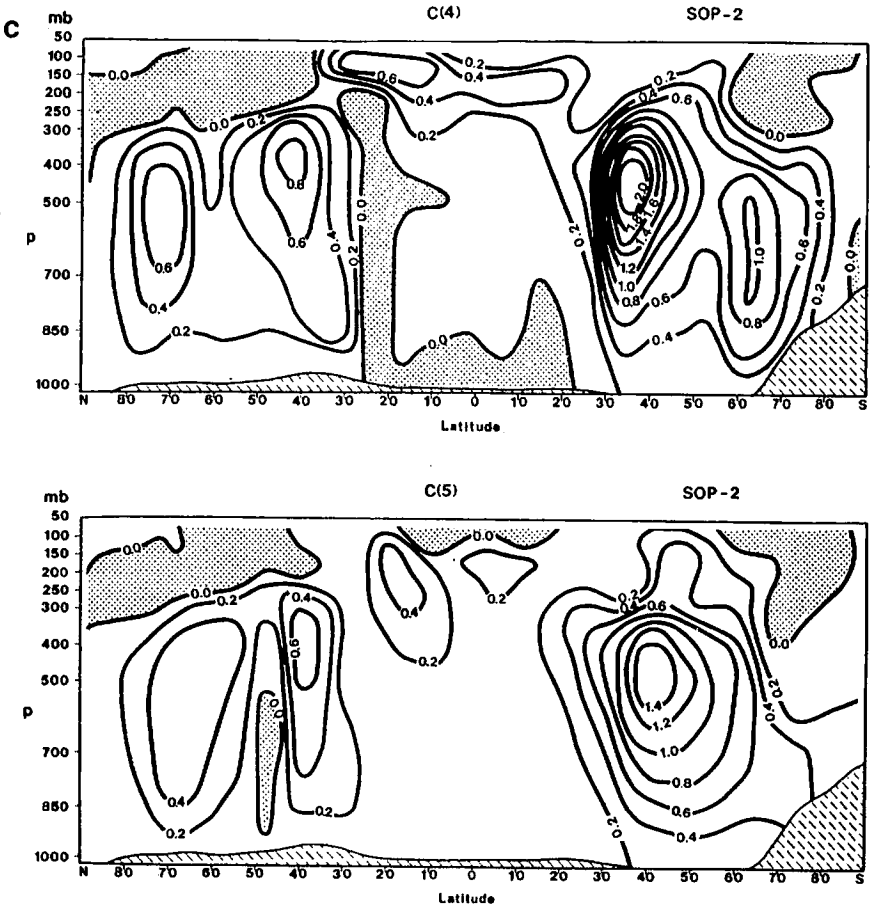

FIG. 9. (*Continued*)

SOP-1 and $n = 9$ for SOP-2, as expected from the activities of the synoptic disturbances. At this scale range, though, the intensity of the conversion is very much weakened, as would be anticipated from the spectral distribution of $C(n)$ in Fig. 1.

Summing up the eddy components of the conversion $C(n)$ over the entire range of computation $n = 1$–30, we obtain the latitude–height cross sections of $-\overline{\omega'\alpha'}$ [i.e., $C(P_E, K_E)$] for SOP-1 and SOP-2, as shown in Fig. 10. In general, the eddy conversion is much more intense during SOP-1 than SOP-2, except for the Antarctic region where strong baroclinic conversion exists during SOP-2. The eddy available potential energy is converted to eddy kinetic energy throughout most latitudes with the maximum in the middle troposphere. During SOP-1 it is interesting to note that positive eddy conversion is identified at most latitudes above the tropopause level, although during SOP-2 the baroclinic conversion is hardly recognized above the tropopause. As shown in Fig. 8, the energy conversion in the lower stratosphere is mostly a contribution from wavenumbers 1, 2 and 3.

6. Concluding remarks

The spectral distribution of the global energy transformations $R(n)$, $M(n)$ and $C(n)$ shows specific seasonal characteristics for SOP-1 and SOP-2. Among these, $R(n)$ shows the largest seasonal variation and $M(n)$ the least. This reflects the sensitive response of the transfer of available potential energy to the thermal field of the seasons. In the long-wave range, $R(n)$ and $C(n)$ are active, while $M(n)$ is active mostly in the long-wave to synoptic-scale ranges. In the shorter-wave range of $n = 11$–15, particularly during SOP-1, $C(n)$ is still significant, reflecting the active synoptic disturbances of the Northern Hemisphere.

There is a maximum production of kinetic energy by $-\mathbf{V} \cdot \nabla\phi$ in subtropical latitudes with a second maximum in high or middle latitudes. The latitude–height cross sections of $-\mathbf{V} \cdot \nabla\phi$ indicate that there is a distinct region of adiabatic destruction of kinetic energy above the lower troposphere in middle latitudes. Kinetic energy convergence $-\nabla \cdot \mathbf{V}k$ is an important additional source of kinetic energy in middle latitudes. The maximum of the dissipation D in middle latitudes is located at latitudes higher than maximum latitudes of $-\mathbf{V} \cdot \nabla\phi$ because of the influx of kinetic energy from lower latitudes. The seasonal contrasts of both $-\mathbf{V} \cdot \nabla\phi$ and D are much more distinct in the Northern Hemisphere than in the Southern Hemisphere. This leads to a more intense global energy transformation during SOP-1 than during SOP-2.

The latitudinal distribution of the cell conversion $-\bar{\omega}''\bar{\alpha}''$ [i.e., $C(0)$], shows its maximum in the equatorial

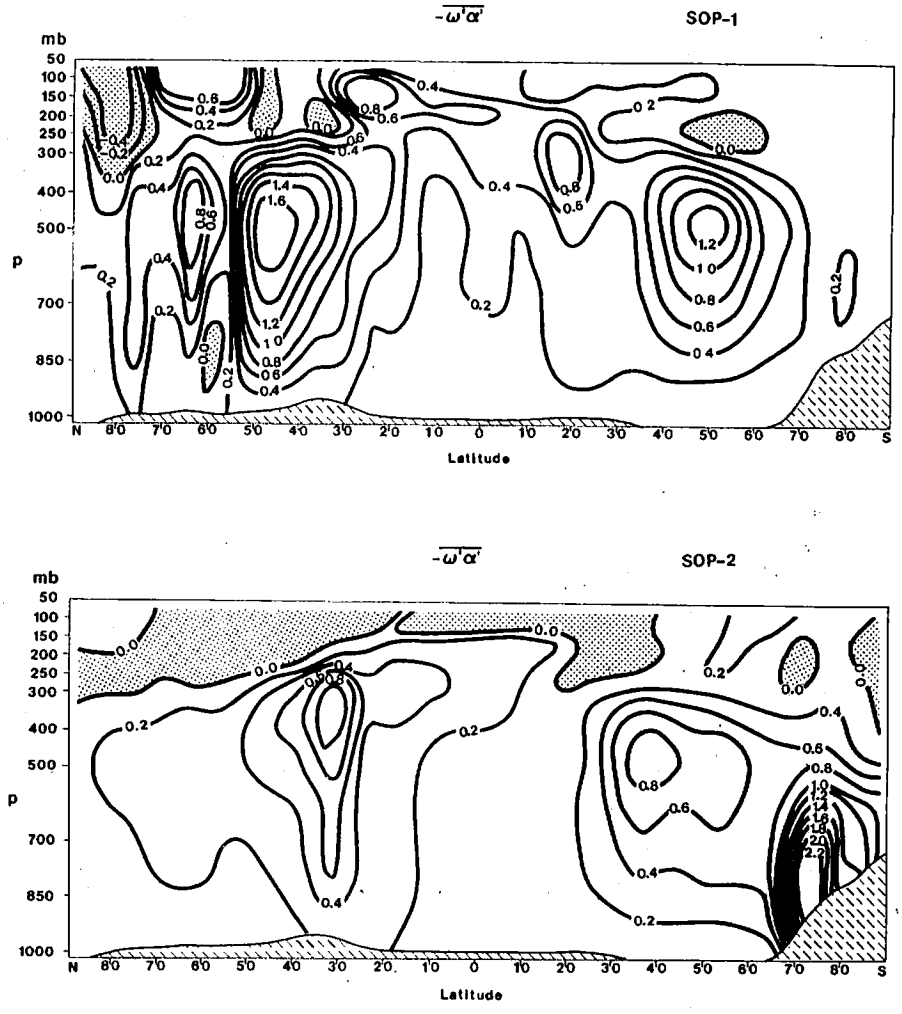

FIG. 10. Latitude-height cross sections of eddy conversion $\overline{\omega'\alpha'}$ [W m^{-2} (100 mb)$^{-1}$] during SOP-1 and SOP-2.

belt where the upward motion of the Hadley cells dominates. The eddy conversion $-\overline{\omega'\alpha'}$ is most intense in middle latitudes of the Northern Hemisphere during SOP-1 in association with the activity of large-scale disturbances. An examination of the spectral conversions $C(n)$ reveals that the conversion by the very long waves $n = 1$, 2 and 3 is intense in middle latitudes of the Northern Hemisphere during SOP-1. During SOP-2 in subtropical to middle latitudes of the Northern Hemisphere, $C(1)$ and $C(2)$ stand out, apparently in relation to the summer monsoon system. In middle latitudes of the Southern Hemisphere the conversion by very long waves is insignificant, and most of the eddy conversion is performed at $n = 4$–6. In the Antarctic region during SOP-2, a strong baroclinic conversion is indicated, with the largest contribution coming from $C(0)$ and $C(1)$.

Acknowledgments. Dr. W. E. Baker of NASA Goddard Laboratory for Atmospheric Sciences is sincerely acknowledged for providing the basic spectral energetics code. The authors appreciate the technical assistance of S. J. Brooks, C. K. Chen, L. K. Gibson, B. G. Miller, R. L. Rees and J. C. Tseng.

This research was supported jointly by the National Science Foundation, the National Oceanic and Atmospheric Administration and the National Aeronautics and Space Administration under GARP Grant ATM-8108216.

REFERENCES

Baker, W. E., E. C. Kung and R. C. J. Somerville, 1977: Energetics diagnosis of the NCAR general circulation model. *Mon. Wea. Rev.*, **105**, 1384–1401.

Kung, E. C., 1967: Diurnal and long-term variation of kinetic energy generation and dissipation for a five-year period. *Mon Wea. Rev.*, **95**, 593–606.

——, 1970: On the meridional distribution of source and sink terms of the kinetic energy balance. *Mon. Wea. Rev.*, **98**, 911–916.

——, and H. Tanaka, 1983: Energetics analysis of the global cir-

culation during the special observation periods of FGGE. *J. Atmos. Sci.*, **40**, 2575–2592.

Lorenz, E. N., 1955: Available potential energy and the maintenance of the general circulation. *Tellus*, **7**, 157–167.

Manabe, S., J. Smagorinsky, J. L. Holloway, Jr. and H. M. Stone, 1970: Simulated climatology of a general circulation model with a hydrologic cycle III: Effect of increased horizontal computational resolution. *Mon. Wea. Rev.*, **98**, 175–212.

Miyakoda, K., J. Sheldon and J. Sirutis, 1982: Four-dimensional analysis experiment during the GATE period. Part II. *J. Atmos. Sci.*, **39**, 486–506.

Newell, R. E., D. G. Vincent, T. G. Dopplick, D. Ferruzza and J. W. Kidson, 1970: The energy balance of the global atmosphere. *The Global Circulation of the Atmosphere*, G. S. Corby, Ed., Roy. Meteor. Soc., 42–90.

Oort, A. H., 1964: On estimates of the atmospheric energy cycle. *Mon. Wea. Rev.*, **92**, 483–493.

——, and J. P. Peixoto, 1974: The annual cycle of the energetics of the atmosphere on a planetary scale. *J. Geophys. Res.*, **79**, 2705–2719.

Peixoto, J. P., and J. A. M. Corte-Real, 1983: The energetics of the general circulation of the atmosphere in Southern Hemisphere during the IGY. Part II: The cycle of the energetics of the atmosphere in Southern Hemisphere. *Arch. Meteor. Geophys. Bioklim.*, **A32**, 1–21.

Saltzman, B., 1957: Equations governing the energetics of the larger scales of atmospheric turbulence in the domain of wavenumber. *J. Meteor.*, **14**, 513–523.

——, 1970: Large-scale atmospheric energetics in the wavenumber domain. *Rev. Geophys. Space Phys.*, **8**, 289–302.

Smith, P. J., and S. Adhikary, 1974: The dissipation of kinetic energy in large-scale atmospheric circulations. *Rev. Geophys. Space Phys.* **12**, 281–284.

Wiin-Nielsen, A., 1968: On the intensity of the general circulation of the atmosphere. *Rev. Geophys. Space Phys.*, **6**, 559–579.